Journal of Manufacturing Processes 34 (2018) 734–739

Contents lists available at ScienceDirect

Journal of Manufacturing Processes

journal homepage: www.elsevier.com/locate/manpro

A new turning system assisted by chip-pulling

Burak Sencer*, Mukhtar Maulimov

Oregon State University, Corvallis, 97331, USA

ARTICLE INFO

Keywords:
Turning
Process control
Monitoring

ABSTRACT

This paper presents a new turning system where the guided cut chip during turning is pulled using an external pulling device to attain high-performance cutting. An electro-mechanical pulling device with sensor-less chip tension monitoring function is designed to steadily pull the guided chip and robustly assist the turning operation. The effect of chip tension on the process is modeled and experimentally verified. The developed chip pulling system is utilized to achieve direct real-time control of the cutting process and zero thrust force cutting is demonstrated. Developed system effectively reduces cutting energy for improved tool life and regulates cutting forces for high performance turning.

1. Introduction

Turning is an efficient cutting process where material removal rates up to 10^4–10^5[cm^3/min] can be achieved [1]. The process is typically controlled by a small set of parameters defining the cutting conditions such as the depth of cut, cutting feed and the speed. Those parameters are selected by the process planner where factors such as tool-workpiece pair, cutting forces, vibrations and tool life [2,3] force a compromise to be made between high material removal rate and machining accuracy/stability. In practice, optimal cutting conditions are determined utilizing process models, through experience and finally by trial and error. In an attempt to deliver greater productivity, cutting process may be tuned adaptively using monitoring information from external or, in-machine sensors [4,5]. However, these approaches are based on adjusting the existing cutting conditions and provide only a limited amount of improvement within the known process limits. The challenge is to exceed the limits to improve efficiency and accuracy of conventional turning by introducing new principles.

Recently, assistive techniques are employed to improve productivity and efficiency of turning process. For instance, laser assisted local heating is applied to improve efficiency of hard turning process [6,7]. Vibration assistance has been applied to various processes, such as drilling [8] turning [9] and grinding [10]. Vibration assistance can help improving process efficiency by facilitating coolant penetration, chip evacuation and even friction control [11]. For instance, elliptical vibration cutting (EVC) [10,12,13] process has been introduced as an enhancement to conventional turning for low speed ultra-precision machining. In EVC, the tool is vibrated elliptically in cutting and chip flow directions. As a result, it reduces the friction effect as the chip flows on the rake face, and thus reduces overall cutting effort (Fig. 1).

Inspired by this, it has been proposed that pulling the cut chip along the rake face during turning can reduce friction forces and thereby improve the cutting process [14]. The concept of chip-pulling cutting is presented in Fig. 2. As shown, if the chip flow could be guided in a controlled manner, an electromechanical device can be used to pull it to cancel the friction force on the rake face. So far, chip pulling has not been realized due to lack of suitable chip flow control methods [15]. Recently, authors proposed a chip guiding method to generate straight continuous chip [16,17]. The method utilizes a cutting insert with guide grooves carved on the rake face to suppress the chip curl and guide it towards a pulling system. This technique has the potential to realize the chip pulling turning process.

In this research, the automated chip-pulling turning process is presented, and the mechanics of this new cutting process is investigated. An electro-mechanical device is developed to continuously pull the cut chip and realize automated chip-pulling turning as shown in Fig. 3. The chip pulling force is introduced as an extra parameter to control the cutting process. Here, regulation of the chip pulling force, i.e. control of the applied chip tension, is critical. A sensor-less approach is favoured and a Kalman Filter [18,19] based disturbance observer technique is designed to estimate chip tension. The effect of chip tension on the process is modelled and experimentally verified. Finally, the chip tension is controlled to achieve high performance turning strategies such as "zero thrust force turning" to achieve precision turning of slender shafts.

Peer-review under responsibility of the scientific committee of NAMRI/SME.

* Corresponding author.
E-mail address: burak.sencer@oregonstate.edu (B. Sencer).

https://doi.org/10.1016/j.jmapro.2018.03.044
Received 11 November 2017; Received in revised form 1 March 2018; Accepted 15 March 2018
Available online 28 June 2018

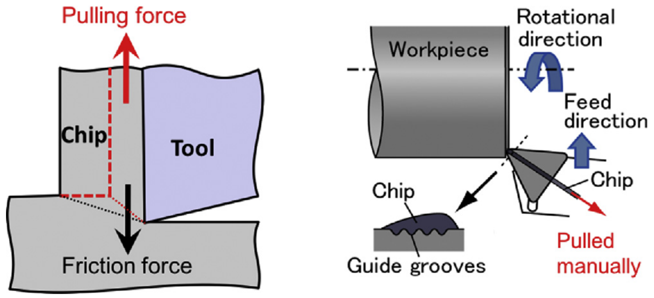

Fig. 1. Friction cancelling (a) and chip pulling turning (b) chip pulling turning concept.

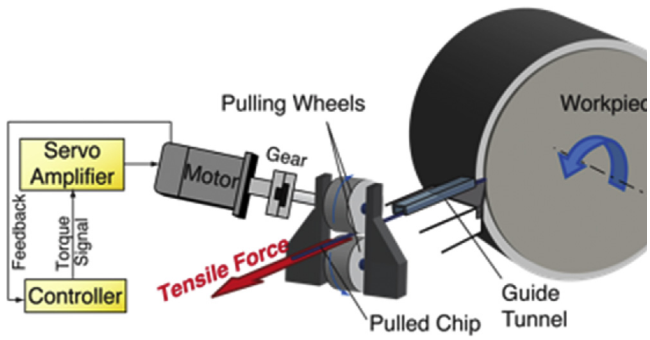

Fig. 2. Automated chip pulling turning process.

2. Development of an electromechanical pulling system for chip pulling turning

2.1. Mechanical design

The automated chip pulling cutting process is presented in Fig. 2. Firstly, a chip guiding system is designed to guide the chip towards the chip-pulling device and realize actual pulling. Fig. 3 shows the chip guiding system [16]. As shown, a tunnel-like structure is utilized to guide the cut chip from the cutting point. Once the cut chip is guided away, it is pulled by a “chip-pulling device” shown in Fig. 4. The pulling device is designed by a pair of rollers driven by servo motor system. Fig. 4(b) depicts the front view and Fig. 4(c) shows top view of the developed pulling device. The working principle of the device is as follows. The chip flows through the tunnel and once it enters in-between the rollers. The friction between the chip and the rollers pull the

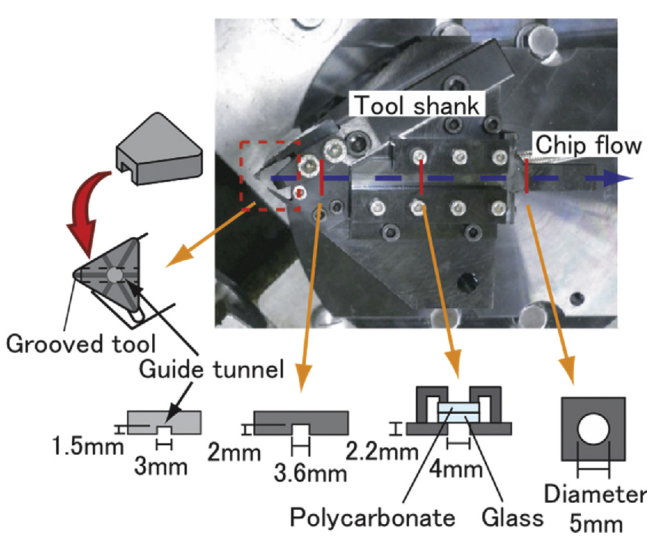

Fig. 3. Chip guiding system.

chip and help apply a tension force. As shown a servo-motor is used to drive the system. The motor torque and speed are controlled by a servo amplifier. The motor torque is transferred to the rollers via a gearbox with a total gear ratio of ½. The rollers are made of hardened steel and their width is 10[mm] with added flanges to restrict the chip escaping from pulling point (See Fig. 4b). In order to be able to smoothly pull the chip through the roller mechanism, the roller speed must be synchronized. This is done mechanically though the designed gearbox. Fig. 4c illustrates the gear-box design. Servo motor drives a master shaft, so-called the “hinge shaft”. Both lower and upper rollers are connected to the shaft with gears (See Fig. 4c). This shaft also serves as a hinge to adjust the gap between rollers. The spacing, i.e. gap, between upper and lower rollers is critical. During pulling, an initial gap between rollers (0.1–0.2[mm]) is set so that guided chip can be taken in easily. As the chip is caught and pulled in by rollers, original chip flow speed is altered. Pulling the chip at a higher speed than its original flow speed reduces the chip thickness. This is simply due to the fact that at a fixed cutting speed, feed and depth, the material removal rate is constant. Therefore, to accommodate continuous chip thickness variation, the gap between rollers must be regulated. This mechanism allows that the upper part of the pulling device, upper roller and associated gears, rotate around the hinge shaft and move the roller slightly up. While doing so, a coil type spring is employed to generate clamping force between the rollers. Clamping force and gap are adjustable where the design can produce up to 314[N] normal force. Considering the steel-to-steel friction coefficient, developed system can generate ~150[N] pulling force at speeds up to 200[m/min].

2.2. Control system

Another challenge is the control of the pulling speed and force. The roller rotation must to be regulated so that the guided chip is pulled gently without breaking it. A straightforward approach is to set the roller speed slightly higher than the original chip flow speed. This would apply a tension on the cut chip. A simple PI (Proportional Integral) speed controller [18] can be used in the servo controller to regulate the roller speed and thereby apply certain chip tension. In order to increase the applied tension, the chip pulling speed, i.e. roller speed, could be increased. Although the relationship is expected to be proportional, it is not necessary linear, and hence the applied pulling force (tension) needs to be monitored so that it does not cause yielding of pulled chip and break it.

The applied tension, in return, generates an equal reaction force on the pulling system. A force sensor or a force dynamometer can be utilized to measure the reaction force. In this work, a sensor-less cost-effective approach is pursued. The reaction force acts as a dynamic disturbance to the speed controller as it tries to resist the roller rotation. This disturbance force can be observed from motor torque and roller speed. A model based Kalman Filter [19] disturbance observer is designed to observe the generated chip tension from noisy roller position measurement and motor torque signal without using an external force sensor. In other words, servo-motor itself is utilized both as an actuator and also a force sensor Fig. 4.

Assuming that the gear mechanism does not have any dominant structural vibration modes, the entire chip pulling system can be modelled considering only the rigid body dynamics. The transfer function between motor torque to roller speed can be written as:

$$v(s) = \frac{1}{J_e s + B_e}[u(s) - F_d(s)],\ x(s) = \frac{1}{s}v(s) \tag{1}$$

where s is the Laplace (s) [18] operator. u[Volts] is torque command to servo drive, v[mm/sec] is the velocity at the pulling point and x[mm] is displacement, i.e. pulled chip length. The control signal equivalent inertia and viscous friction in the puling system are identified as $J_e = 3.13 \times 10^{-4}$[V/(mm/sec^2)] and $B_e = 5.39 \times 10^{-4}$[V/(mm/sec)] trough tests. F_d[V] represents the control signal equivalent lumped

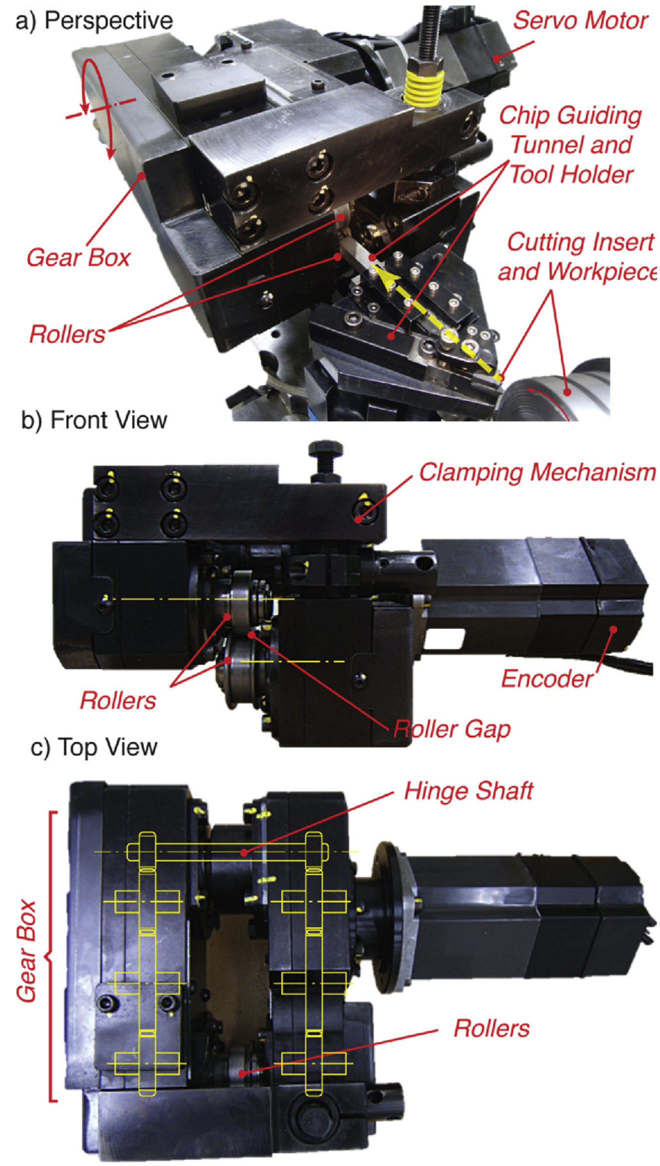

Fig. 4. Developed chip pulling device.

disturbances acting against the roller rotation. It is reasonable to assume that they are dominated by chip tension F_{pull} and also constant coulomb friction that is pre-identified to be $F_c = 1.41$[V]. Notice that coulomb friction is assumed to be static [20,21] in this system. In precision motion systems, comprehensive dynamic friction models such as the Stribeck type regimes should be considered [22] to be able to acquire more accurate disturbance observation. Eq. (1) is then converted to state-space form as:

$$\begin{bmatrix} v(t)\\ \dot{v}(t)\end{bmatrix} = \mathbf{A_c}\begin{bmatrix} x(t)\\ v(t)\end{bmatrix} + [\mathbf{B_c} - \mathbf{B_c}]\begin{bmatrix} u(t)\\ F_d(t)\end{bmatrix},\quad \mathbf{A_c} = \begin{bmatrix} 0 & 1\\ 0 & \frac{-B_e}{J_e}\end{bmatrix},\ \mathbf{B_c} = \begin{bmatrix} 0\\ \frac{1}{J_e}\end{bmatrix} \tag{2}$$

and discretised at sampling interval of the servo control system at T_s=1[msec] to derive the state transition matrices, $\mathbf{A_d} = e^{\mathbf{A_c}T_s}$ and $\mathbf{B_d} = \int_0^{T_s} e^{\mathbf{A_c}\tau}d\tau\cdot\mathbf{B_c}$. Considering the quantized encoder measurement $\tilde{x}$ and sampled motor torque signal, $\tilde{u}$ the augmented discrete state-space model is postulated as:

$$\left.\begin{aligned}
&\begin{bmatrix} x(k+1)\\ \omega(k+1)\\ F_d(k+1)\end{bmatrix} = \mathbf{A}\begin{bmatrix} x(k)\\ \omega(k)\\ F_d(k)\end{bmatrix} + \mathbf{B}[u(k-1)] + \mathbf{W}\begin{bmatrix}\tilde{u}(k)\\ \widetilde{w}_d(k)\end{bmatrix}\\
&[x_m(k)] = \mathbf{C}\begin{bmatrix} x(k)\\ \omega(k)\\ F_d(k)\end{bmatrix} + \mathbf{V}[\tilde{x}(k)],\ \text{where}\\
&\mathbf{A} = \begin{bmatrix}\mathbf{A_d} & -\mathbf{B_d}\\ \mathbf{0}_{1\times 2} & 1\end{bmatrix},\ \mathbf{B} = \begin{bmatrix}\mathbf{B_d}\\ 0\end{bmatrix},\ \text{and}\\
&\mathbf{C} = \begin{bmatrix}1\\0\\0\end{bmatrix},\ \mathbf{W} = \begin{bmatrix}\mathbf{B_d} & \mathbf{0}_{2\times 1}\\ 0 & 1\end{bmatrix},\ \mathbf{V} = 1
\end{aligned}\right\} \tag{3}$$

where *ω(k)* is sampled velocity. In this Kalman Filter formulation, the slowly varying disturbances, e.g. F_d, is considered as an extra state and the original system from Eq. (3) is augmented through the use of a perturbation variable, w_d. The amount of perturbation, i.e. variation, in disturbance state will be used as a tuning parameter to control the bandwidth, i.e. speed, of the Kalman Filter and observation of the chip tension. Higher values give more accurate pulling force estimates; however, they become more polluted with noise. Finally, Eq. (3) facilitates design of a full-state observer where quantization noise in position measurements are considered and both filtered position, and velocity signals are generated as follows:

$$\left.\begin{aligned}
&\underbrace{\begin{bmatrix}\hat{x}(k)\\ \hat{\omega}(k)\\ \hat{F}_d(k)\end{bmatrix}}_{\text{state estimations}} = [\mathbf{I} - \mathbf{K}_{\mathbf{obs}}\mathbf{C}]\mathbf{A}\begin{bmatrix}\hat{x}(k-1)\\ \hat{\omega}(k-1)\\ \hat{F}_p(k-1)\end{bmatrix} +\\
&[\mathbf{I} - \mathbf{K}_{\mathbf{obs}}\mathbf{C}]\mathbf{B}\underbrace{[u(k-1)]}_{\text{torque command}} + \mathbf{K}_{\mathbf{obs}}\underbrace{[x_m(k)]}_{\text{measurements}}
\end{aligned}\right\} \tag{4}$$

Above, $\boldsymbol{K_{obs}}$ is the Kalman observer gain. It is determined from noise variances [19] of position and control signals, and by tuning the disturbance perturbation variance. Further details on calculation of Kalman Filter gain can be found in [20]. Corresponding natural frequencies and damping ratios for the observer poles are computed from the eigenvalues of the disturbance dynamics $p_{1,2,3} = eig(\mathbf{I} - \mathbf{K_{obs}})\mathbf{A}$ as:

$$\left. p_1 = 5[\text{rad/sec}], p_{2,3} = 119[\frac{rad}{\text{sec}}],\ \zeta = 0.995\right\} \tag{5}$$

Once the control signal equivalent disturbance signal is calculated from Eq. (3), identified static coulomb friction is subtracted, $F_{pull} \approx F_d - F_c$, and scaled by the force coefficient of the servo system $K_t = 43$[N/V] to compute chip tension in real time.

2.3. Automated chip pulling by the developed pulling system

The effect of chip pulling on turning process and functionality of the developed chip pulling system is demonstrated experimentally. Turning experiments are conducted at 2 different pulling speeds and summarized in Fig. 5. Firstly, the original chip flow speed is measured from conventional cutting tests. Low carbon steel (S10C) is cut at 76.7[m/min], and the original, i.e. free, chip flow speed is observed as 16[m/min] (See Fig. 5). Chip pulling-cutting is then performed by setting the roller speed to 20[m/min] and 35[m/min], respectively to insert pulling force. As shown in Fig. 5, once the chip is guided, it enters the pulling device within 1[sec] from the start of cutting and pulled smoothly without breaking it. By forcing the chip flow speed 1.25 times higher than its original value, i.e. pulling at 20[m/min], cutting forces are influenced only slightly. By increasing the chip pulling speed roughly 2 times higher than its original flow speed, cutting forces could be reduced (See Fig. 5). Note that the effect of chip pulling can be observed clearly from the friction force component and the friction angle of the process. Here, the resultant friction force component is defined as the original friction force subtracted by the pulling force, and

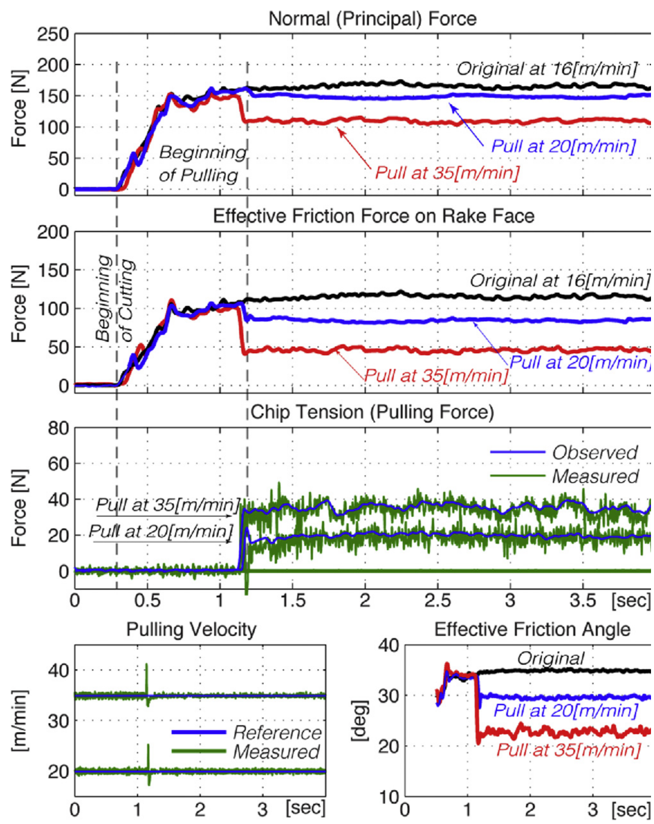

Fig. 5. Chip pulling turning using developed pulling system. (Workpiece: low-carbon steel (JIS: S10C), Tool: cermet insert with guide grooves, nose radius of 0.4[mm] and rake angle of 0[deg], Feed: 0.16[mm/rev], Rotational speed: 215[rpm], Depth of cut: 0.3[mm]).

it is used to compute the friction angle. As shown in Fig. 5 the effective friction angle could be reduced from 35[deg] to 22[deg].

The performance of the chip tension observer is also validated in Fig. 5. The actual chip tension (pulling force) is measured through a Kistler force rings mounted under the pulling device. As shown in Fig. 5, Kalman Filter disturbance observer structure can observe slowly varying chip tension accurately from noisy signals. Hence, it provides a cost-effective means of observing chip tension enabling sensor-less operation that is suitable for industrial implementation and also facilitates design of a force controller for direct chip tension regulation.

3. Chip pulling turning process model

The effect of chip pulling in turning process is demonstrated briefly in the previous section. As compared to conventional turning, in chip-pulling turning, process forces can be minimized by applying tension on the cut chip by cancelling the friction forces as depicted in Figs. 1 and 2, and also experimentally demonstrated in Fig. 5. It allows real-time control of friction and shear angles without changing any of the cutting process parameters. This section models effect of chip pulling on the process based on the orthogonal cutting theory [1,23] based on the single thin shear plane model.

Assuming a thin shear plane, a cutting force diagram is drawn for chip pulling cutting as depicted in Fig. 6. Firstly, when the chip is pulled, pulling force directly cancels friction force on the rake face by the amount of F_{pull}, which rotates the resultant force direction (See Fig. 6). Since shear deformation occurs by the resultant force, the shear direction also rotates creating a larger shear angle, φ'. The new shear plane has a smaller shear area due to increased chip thickness ratio. Normal and friction forces are reduced to F_n' and f' as depicted in Fig. 6. In contrast, friction angle does not change significantly and is assumed

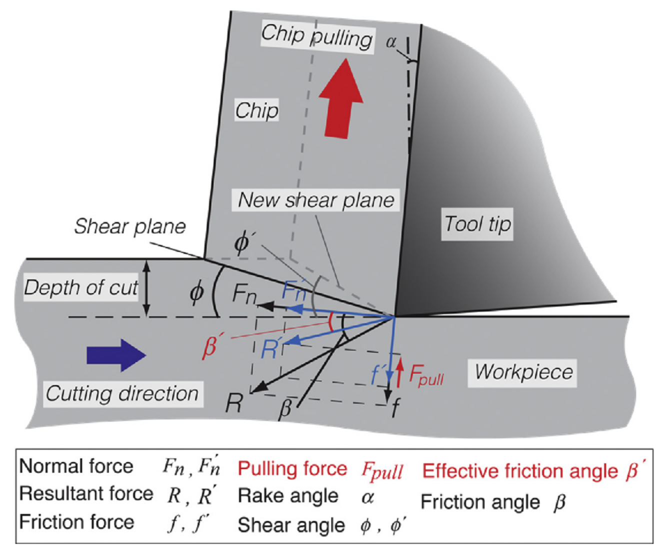

Fig. 6. Force diagram for chip pulling cutting model.

to be constant as a property of the material-tool pair [1]. Since chip pulling force cancels friction force, the deducted friction force f'-F_{pull} defines a new friction angle β' and a resultant force vector, R'. It should be noted that β' is defined as the "effective friction angle" associated with the chip pulling cutting process, and it can be manipulated by the pulling force.

Thus, the idea of "effective friction angle", β', allows incorporation of the pulling force to the well-known orthogonal cutting model and facilitate analysis of the process. Firstly, maximum shear stress or minimum energy principle [23],

$$\phi' = 45^0 + \alpha - \beta' \quad \text{or} \quad \phi' = 45^0 + \alpha/2 - \beta'/2 \tag{6}$$

can be used to predict the modified shear angle. The resultant force of the new process is calculated from shear strength τ_s and cutting area A as:

$$R' = \frac{\tau_s A}{\sin(\phi')\cos(\phi' - \alpha + \beta')} \tag{7}$$

The relationship between normal and friction forces are obtained from the force diagram (see Fig. 6) and Eq. (7):

$$\left.\begin{aligned} F_n' &= R'\cos(\beta') \\ f' &= R'\cos(\beta')\tan(\beta) \end{aligned}\right\} \tag{8}$$

Using above relationships, pulling force to achieve the desired effective friction angle is calculated as:

$$F_{pull} = \frac{\tau_s A}{\sin(\phi')\cos(\phi' - \alpha + \beta')}[\cos(\beta')\tan(\beta) - \sin(\beta')] \tag{9}$$

Eq. (9) defines the required chip tension to control the effective friction angle and thus the cutting process. The model is evaluated at various pulling conditions where simulated cutting forces, cutting energy and the required pulling effort are compared to actual measurements. Note that, accuracy of max. shear stress and min. energy principle models depend heavily on cutting conditions. Given the zero-rake angle condition and simplicity of the Merchant's model as shown in Fig. 7, both max. shear stress and min. energy principles actually capture the chip-pulling process mechanics well. Both models validate that introducing controlled tension on the chip; process forces could be reduced almost by half without changing any of the actual cutting parameters. It introduces an opportunity to cut in higher material removal rate and efficiency with lower forces. In particular, for certain processes thrust force can be cancelled completely by the pulling force for precision or chatter-free cutting of flexible work-pieces, which is demonstrated in

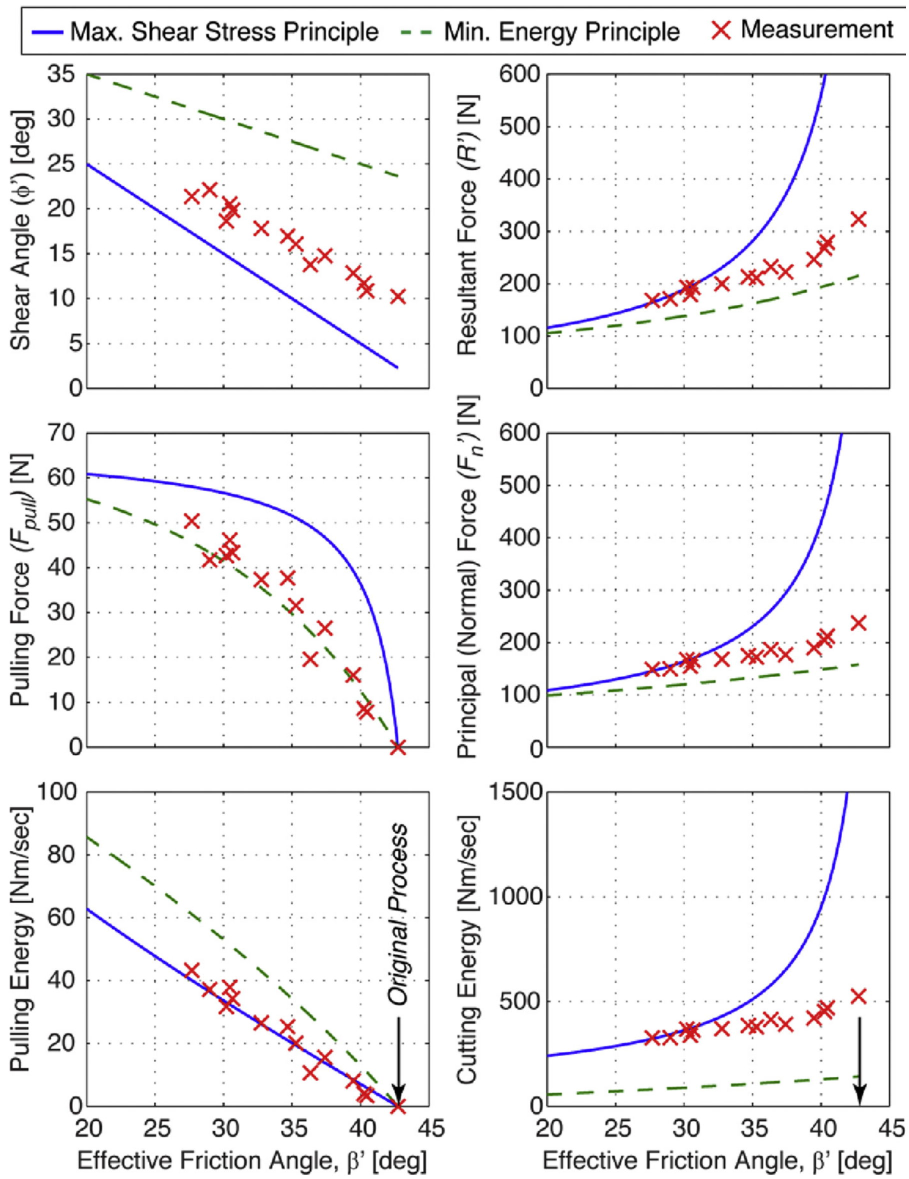

Fig. 7. Analytical and experimental results of chip pulling turning process. (Workpiece: low-carbon steel (JIS: S10C), Tool: sintered tungsten carbide insert with guide grooves, nose radius of 0.8[mm] and rake angle of 0[deg], Feed: 0.12[mm/rev], Rotational speed: 215[rpm], Cutting speed: 133 [m/min], Depth of cut: 0.4[mm]).

the following section. As the pulling force is increased, friction energy consumed by cutting is reduced. The advantage obtained in reduction of cutting energy is more than 5 times than that of inputted by pulling. This in return reduces overall energy, heat generation and helps to improve tool life.

4. High performance turning with the developed system

In conventional turning processes the thrust force component acts in the radial direction and therefore causes deflection errors or chatter vibrations on slender/thin compliant workpieces. If adjusted correctly, the chip pulling force can be used to reduce friction force on rake face to achieve zero thrust force cutting as well. Note that if the pulling force is greater than then friction force, workpiece can even be pulled towards the tool generating negative friction force component. This characteristic is actually similar to the mechanics elliptical vibration cutting process [13].

Here, a preliminary application is considered, and results are demonstrated in Fig. 8. In this experiment compliant soft copper workpiece is machined with a PCD tool. As shown, friction force on the tool is cancelled by the pulling force that is controlled by the developed chip tension control system. This, in return, allows cancellation of the thrust force component and enables precision finish of slender shafts without deflection and circumventing vibration problems [24,25].

5. Conclusions

This paper presented a new turning process that is enhanced by pulling the cut chip. An electromechanical pulling system is designed for automatically pulling the chip. A sensor-less pulling force monitoring function is designed to gently apply tension on the guided cut chip and to attain high performance turning. It is shown that develop chip pulling system can pull the chip at different speeds and apply controlled tension to cancel friction forces and thereby improve the process efficiency. The system demonstrated that the friction force can be fully cancelled to achieve precision turning of slender workpieces. Lastly, the thin shear plane model is utilized to model the mechanics of the chip pulling cutting process. The model captures the fundamental effect of chip pulling reasonably well and provides guidance for planning the process.

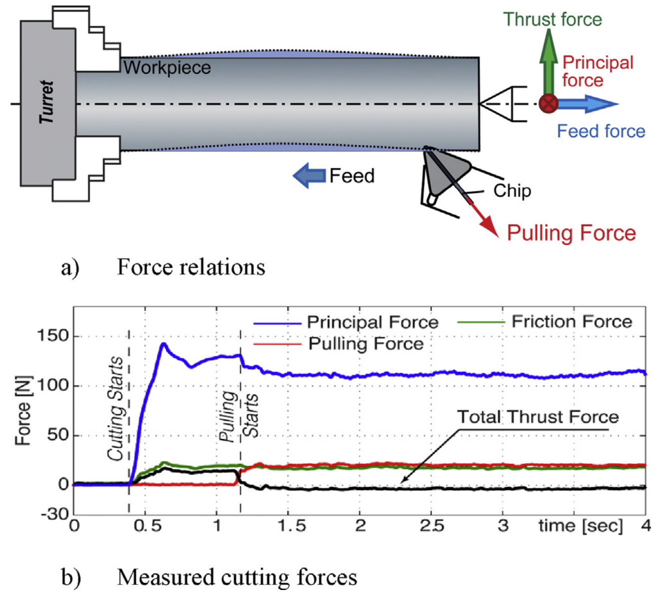

Fig. 8. Zero thrust force control. (Workpiece: tough pitch copper, Tool: PCD insert with a guide groove, nose radius of 0.8[mm] and rake angle of 0[deg], Feed: 0.12[mm/rev], Rotational speed: 315[rpm], Depth of cut: 0.6[mm], Cutting speed: 65[m/min]).

Acknowledgements

This research is supported by NSF's Academic Liaison with Industry (GOALI) Award Number: 1661926.

Authors express their deep gratitude to the Manufacturing Engineering Laboratories of Nagoya University, Japan.

References

[1] Altintas Y, Weck M. Chatter stability in metal cutting and grinding. Ann CIRP 2004;53/2:619–42.
[2] Merdol SD, Altintas Y. Virtual simulation and optimization of milling applications—part II: optimization and feedrate scheduling. ASME J Manuf Sci Eng 2008;130(5):051005.
[3] Wang H, Jang P, Stori JA. A metric-based approach to two-dimensional (2D) tool-path optimization for high-speed machining. ASME J Manuf Sci Eng 2005;127(1):33.
[4] Liang SY, Hecker RL, Landers RG. Machining process monitoring and control: the state-of-the-art. Trans ASME J Manuf Sci Eng 2004;126/2:297–310.
[5] Kakinuma Y, Sudo Y, Aoyama T. Detection of chatter vibration in end milling applying disturbance observer. Ann CIRP 2011;60/1:109–12.
[6] Bejjani R, Shi B, Attia H, Balazinski M. Laser assisted turning of titanium metal matrix composite. CIRP Ann Manuf Technol 2011;60(1):61–4.
[7] Melkote S, Kumar M, Hashimoto F, Lahoti G. Laser assisted micro-milling of hard-to-machine materials. CIRP Ann – Manuf Technol 2009;58(1):45–8.
[8] Ladonne M, Cherif M, Landon Y, K'Nevez JY, Cahuc O, de Castelbajac C. Modelling the vibration-assisted drilling process: identification of influential phenomena. Int J Adv Manuf Technol 2015;81(9–12):1657–66.
[9] Peng Y, Wu YB, Liang ZQ, Guo YB, Lin X. An experimental study of ultrasonic vibration-assisted grinding of polysilicon using two-dimensional vertical workpiece vibration. Int J Adv Manuf Technol 2011;54(9):941–7.
[10] Shamoto E, Moriwaki T. Study on elliptical vibration cutting. Ann CIRP 1994(43/1):35–8.
[11] Brehl DE, Dow TA. Review of vibration-assisted machining. Precis Eng 2008;32(3):153–72.
[12] Kim J-D, Lee E-S. A study of ultrasonic vibration cutting of carbon fibre reinforced plastics. Int J Adv Manuf Technol 1996;12(2):78–86.
[13] Shamoto E, Moriwaki T. Ultaprecision diamond cutting of hardened steel by applying elliptical vibration cutting. CIRP Ann - Manuf Technol 1999;48(1):441–4.
[14] Nakayama K. Effect of tension applied to chip during metal cutting. Bull. JSPE 1964;30/1:46–51.
[15] Jawahir IS, Van Luttervelt CA. Recent developments in chip control research and applications. Ann CIRP 1993;42/2:659–93.
[16] Shamoto E, Aoki T, Sencer B, Suzuki N, Hino R, Koide T. Control of chip flow with guide grooves for continuous chip disposal and chip-pulling turning. Ann CIRP 2011;60/1:125–8.
[17] Aoki T, Sencer B, Shamoto E, Suzuki N, Koide T. Development of a high-performance chip-guiding turning process—tool design and chip flow control. Int J Adv Manuf Technol 2016;85(1-4):791–805.
[18] Dorf RC, Bishop RH. Modern control systems. Pearson; 2011.
[19] Kalman RE. A new approach to linear filtering and prediction problems. J Basic Eng Trans ASME 1960;82:35–44.
[20] Erkorkmaz K, Altintas Y. High speed CNC system design: part II. Int J Mach Tools Manuf 2001;41/10:1487–509.
[21] Olsson H, Åström KJ, De Wit CC, Gäfvert M, Lischinsky P. Friction models and friction compensation. Eur J Control 1998;4(3):176–95.
[22] IEEE. Dupont P, Armstrong B, Hayward V. Elasto-plastic friction model: contact compliance and stiction. American Control Conference, 2000. Proceedings of the 2000 (Vol. 2, pp. 1072–1077 2000.
[23] Shamoto E, Altintas Y. Prediction of shear angle in oblique cutting with maximum shear stress and minimum energy principles. ASME J Manuf Sci Eng 1999;121(3):399–407.
[24] Budak E, Altintas Y. Analytical prediction of chatter stability in milling—part II: application of the general formulation to common milling systems. J Dyn Syst Measur Control 1998;120(1):31–6.
[25] Altintas Y, Weck M. Chatter stability of metal cutting and grinding. CIRP Ann-Manuf Technol 2004;53(2):619–42.